

# Synchrotron radiation-based micro computed tomography in the assessment of dentin de- and re-mineralization

Florian Kernen<sup>a,b,c</sup>, Tuomas Waltimo<sup>c</sup>, Hans Deyhle<sup>a</sup>, Felix Beckmann<sup>d</sup>, Wendelin Stark<sup>e</sup>, and Bert Müller<sup>\*a,b</sup>

<sup>a</sup>Institute of Materials Science, Dental School, University of Basel, Switzerland;

<sup>b</sup>Biomaterials Science Center, University of Basel, Switzerland;

<sup>c</sup>Institute of Preventive Dentistry and Oral Microbiology, Dental School, University of Basel Switzerland;

<sup>d</sup>GKSS-Research Center Geesthacht, Germany;

<sup>e</sup>Department of Chemistry, ETH Zürich, Switzerland

## ABSTRACT

Synchrotron radiation-based micro computed tomography (SR $\mu$ CT) is well established to determine the degree of mineralization in bony tissue. The present study demonstrates that the method can be likewise used for three-dimensional analyses of dentin de- and remineralization. Four dentin discs about 4 mm in diameter and 0.8 mm thick were prepared from freshly extracted human third molars. In order to study the de- and re-mineralization, three of them were treated with 10% citric acid for the period of 10 min. Nano-particulate bioactive glass made of SiO<sub>2</sub>, P<sub>2</sub>O<sub>5</sub>, CaO, Na<sub>2</sub>O served for the re-mineralization in physiological saline. This process was carried out at the incubation temperature of 37 °C for 1 and 7 d, respectively. The native and the treated discs were comparatively examined by SR $\mu$ CT in absorption contrast mode. Already the visual inspection of the tomograms obtained reveals remarkable differences related to the mean X-ray absorption and internal microstructure. The de-mineralization led to a surface morphology characteristic for the treated dentin collagen matrix. The re-mineralized discs show a dependence on the period of the treatment with the bio-active glass suspension. Initial signs of the remineralization were clearly present already after 24 h of incubation. The disc incubated for 7 d exhibits a degree of mineralization comparable to the native control disc. Thus, SR $\mu$ CT is a powerful non-destructive technique for the analysis of dentin de- and re-mineralization.

**Keywords:** Bio-active glass, dentin de- & re-mineralization, synchrotron radiation, micro computed tomography

## 1. INTRODUCTION

Since the introduction in the 1970s, bio-active glasses have been applied to treat a great variety of medical indications. The surfaces of these materials allow for direct bonding to hard and soft tissues.<sup>1</sup> In dentistry, bio-active glasses have been used to augment alveolar ridges, to treat periodontal pockets, and to treat dentin hypersensitivity.<sup>2-4</sup> Dentin consists of a collagen matrix, which is mainly mineralized by hydroxylapatite (HA) crystallites. The dentin structure and density depends on its location. For example, the number and size of tubules, the microscopic channels, which radiate throughout dentin, change from the periphery towards the pulp chamber (cp. Figure 1). Near pulp, the tubules are two to three micrometers wide and have a high density, whereas close to the dentin-enamel junction, the tubules are less than one micrometer and exhibit a relatively low density. Here, they occupy less than 1% of the cross section. In the dental crown, the direction of dentinal tubules is generally perpendicular to the dentin-enamel junction, whereas in the root the dentinal tubules are laterally oriented from the root canal. Thus, depending on the location within the tooth, the degree of dentin mineralization varies remarkably. In addition, the degree of dentin mineralization depends on the developmental stage of the tooth.<sup>5</sup> Moreover, the inter-individual variation in the level of mineralization is obvious. Hence, attention has to be paid to the heterogeneity in studies on the dentin mineralization as often performed by conventional histology.

---

\* Further author information: [bert.mueller@unibas.ch](mailto:bert.mueller@unibas.ch)

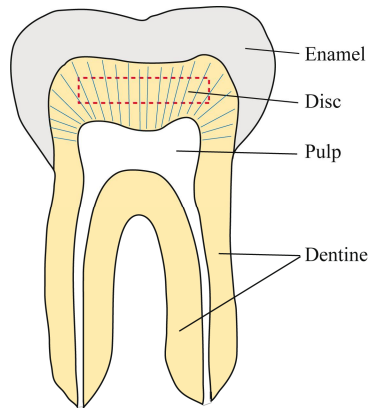


Fig. 1. The scheme of the human molar tooth shows the general anatomy as well as the location of the extracted dentin discs. Usually, one can obtain only one to two disks per tooth, each about 1 mm thick. The density and mineral content and, therefore, the X-ray absorption are expected to depend on the relative distance from the pulp and enamel junctions.

Bio-active glasses of the well known  $\text{SiO}_2\text{-Na}_2\text{O-CaO-P}_2\text{O}_5$  system suspended in aqueous solutions release their ionic compounds.<sup>6, 7</sup> The release of sodium and calcium ions from and the incorporation of  $\text{H}_3\text{O}^+$  into the corroding glass results in a basic environment, intolerable for most oral micro-organisms.<sup>7-10</sup> In contrast to commonly used disinfectants in dentistry, silica-containing bio-active glasses induce dentin mineralization and the formation of calcium phosphate precipitations.<sup>11, 12</sup> Thus, bio-active glasses are promising candidates for dressings on infected and de-mineralized dentin found in profound carious lesions and necrotic root canals. Detailed, quantitative data on the re-mineralization capacity, however, are rare and may depend on patient-specific situations. Therefore, it is desirable to develop techniques that support the quantification of de- and re-mineralization processes of teeth. Synchrotron radiation-based micro computed tomography (SR $\mu$ CT) allows nondestructively measuring the local X-ray attenuation coefficients. Besides the X-ray energy dependence, it is well established that the X-ray absorption strongly depends on the atomic number and on the density of the material. Consequently, the local absorption of the monochromatic X-ray beam might be used to uncover the degree of mineralization or even to determine the distribution of calcium phosphate phases in the dentin specimens.

The present communication describes the approach to detect de- and re-mineralization of dentin specimens *in vitro* by SR $\mu$ CT. It can be expected that sophisticated algorithms are necessary for the appropriate analysis since the effects of de- an re-mineralization might mainly occur at the surfaces of the dentin disks, which could be even anisotropic and inhomogeneous concerning microstructure and calcium distribution. Specifically, we report here the assessment of the re-mineralization of artificially de-mineralized dentin specimens, which have been exposed to an aqueous suspension of the nanoparticulate bio-active glass 45S5.

## 2. MATERIALS AND METHODS

### 2.1 Specimen preparation

Four dentin discs were mechanically removed from freshly extracted human third molars using a trephine bur cylinder with a diameter of 4 mm. Subsequently, the discs, with a thickness of 0.8 mm, were cut from the dentin section of the cylinder using the saw microtome (SP1600; Leica, Wetzlar, Germany). The discs were autoclaved at a temperature of 121 °C for 15 min before storage in sterile saline solution at a temperature of 5 °C. Three of the four discs were de-mineralized using 10% citric acid (University pharmacist, Zürich) at room temperature for a period of 10 min. Experimental flame spray-derived nanoparticulate bio-active glass  $\text{SiO}_2$  (47.8%),  $\text{P}_2\text{O}_5$  (4.6%), CaO (25.1%),  $\text{Na}_2\text{O}$  (22.6%) (NanoBAG, Department of Chemistry, ETH Zürich) was suspended in physiological saline (1:5 wt/vol). For the re-mineralization, two of the three de-mineralized specimens were incubated in the suspension at a temperature of 37 °C for 24 h and 7 d, respectively. Therefore, in addition to the controls, i.e. the native unchanged disc and the de-mineralized one, two re-mineralized specimens were generated, which differ only in the duration of the re-mineralization treatment. The specimens were labeled according to the numbering given in Table 1.

Table 1. Labeling of the specimen according to their de- and re-mineralization treatment.

Specimen	De-mineralization	Re-mineralization
Disc 1	No treatment	No treatment
Disc 2	Citric acid at 37 °C for 10 min	No treatment
Disc 3	Citric acid at 37 °C for 10 min	NanoBAG 45S5 at 37 °C for 24 h
Disc 4	Citric acid at 37 °C for 10 min	NanoBAG 45S5 at 37 °C for 7 d

## 2.2 SR $\mu$ CT measurements

For the SR $\mu$ CT data acquisition, the four discs were placed into one Eppendorf container 5 mm in diameter. To maintain physiological conditions, the container was filled with saline solution. This container was glued onto the holder for the high-precision rotation stage.

The 1441 projections were recorded at the beamline W 2 (HASYLAB at DESY, Hamburg, Germany) using the standard tomography set-up for absorption contrast mode that is operated by the GKSS-Research Center.<sup>13</sup> In order to realize a high spatial resolution, the projections were recorded in the following way.<sup>14</sup> First, the rotation axis was shifted by 1.4 mm to an asymmetric position. Rotating the specimen by 360°, two projections could be merged with pixel precision to finally feed the projections into the conventional filtered back-projection algorithm.<sup>15</sup> Second, two tomograms obtained at different height levels (shift 2.0 mm) were combined again with pixel size precision. Hence, a voxel size of 2.13  $\mu\text{m}$  could be reached. The spatial resolution of the entire set-up (7.76  $\mu\text{m}$ ) was determined by means of a metallic edge as described previously.<sup>16</sup> After a first scan, performed with the photon energy of 40 keV, did not provide satisfactory contrast, a scan with the photon energy of 27 keV was used to obtain the data presented here, as it better fits the criteria derived by Grodzins.<sup>17</sup>

## 2.3 Data treatment

The visualization software VG Studio Max 1.2.1 (Volume Graphics, Heidelberg, Germany) served for the three-dimensional visualization of the tomography data. Because of the data size and to improve contrast,<sup>18</sup> tomograms with different binning factors were generated. Here, 4, 9, and 16 pixels were merged in the projections prior to the reconstruction to attain binning factors of 2, 3, and 4, respectively.

For the quantitative analysis of the different discs and parts of the discs such as rim and core, the tomograms were rotated so that it became possible to easily crop the region of interest. Further tools, also based on the interactive data language (IDL Research Systems Inc., USA), were developed for cropping and histogram read-out.

# 3. RESULTS

## 3.1 Characterization of dentin mineralization by histogram analysis

Figure 2 shows a histogram of the local absorption values from the entire tomogram with the binning factor of 4. This histogram exhibits several peaks. In order to identify their origin, a virtual cut was colored according to the bar in the histogram. It becomes obvious that the light blue corresponds to the air, the dark blue to the polymer of the Eppendorf container, violet to the saline solution and yellow to red to the lower absorbing parts of the discs as well as black to the highly absorbing parts of the discs. The relatively small, green-colored peak does not represent one medium but originates from partial volume phenomena. For the investigation of the mineralization, only absorption levels above 2  $\text{mm}^{-1}$  are of interest, which facilitates the intensity-based segmentation of the dentin discs.

The histograms of the segmented discs are shown in Figure 3. They are restricted to the local absorption levels of dentin at the photon energy of 27 keV that correspond to values between 2.5 and 4.5  $\text{mm}^{-1}$ . At first glance, the native disc (Disc 1) should exhibit the higher degree of mineralization with respect to the etched one (Disc 2) and, therefore, the peak in the histogram should be shifted to higher X-ray absorption levels. Here, however, we observe the opposite behavior. Disc 2 presents a 5% higher local absorption compared to the other three discs.

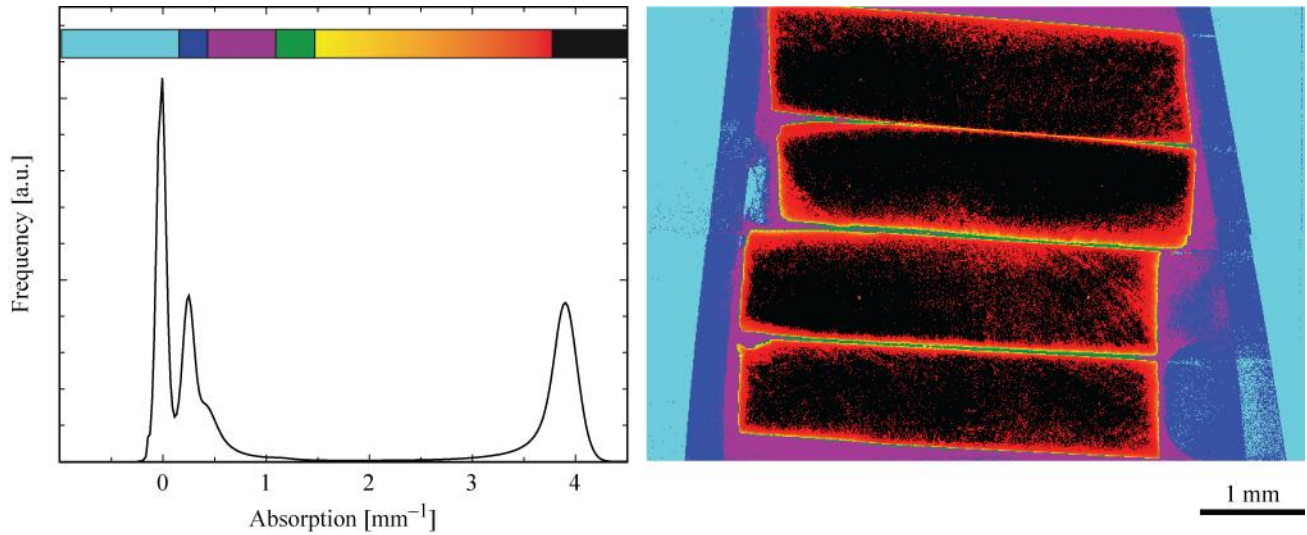


Fig. 2. On the left, the histogram of the local absorption values from the collected tomography data is represented. Using the color table as indicated by the color bar in the histogram one obtains the selected virtual cut on the right. The four dentin discs are easily identified and match to Disk 1 to 4 from top to bottom.

The histograms of the dentin discs do not show the Gaussian shape often observed for the SR $\mu$ CT-measurements.<sup>19</sup> The asymmetry of the peaks in the histograms is characteristic for the composite materials with density variations, and the related X-ray absorption modulations, on true micrometer scale.

Furthermore, the degree of mineralization seems to be asymmetric and higher on one side, as clearly seen for Disc 1 and Disc 2 in the colored slice of Figure 2. To obtain a quantitative estimate of the asymmetry, the absorption value histograms of the outer region (top and bottom, respectively) were compared with the ones from the core of the discs as illustrated for Disc 2 in Figure 4. This procedure presents numerous difficulties, since any value crucially depends on the choice of the region of interest and the definition of the peak position. Nevertheless, the data obtained correspond well to the visual impressions. They are summarized in Table 2. Disc 1 and Disc 2 provide asymmetries of more than 10%, whereas Disc 3 and Disc 4 are symmetric.

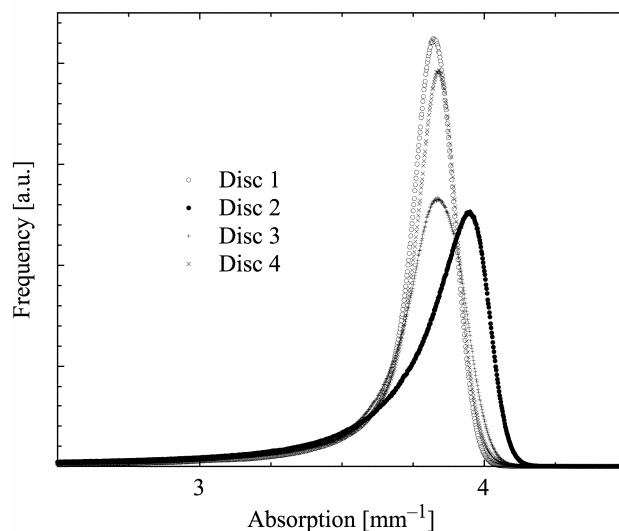


Fig. 3. The histogram of the local absorption values between 2.5 and 4.5  $\text{mm}^{-1}$  from the individual discs shows the highest level for the etched disc (Disc 2). The asymmetry of the peaks reflects the composite character of dentin with density variations on the micrometer scale.

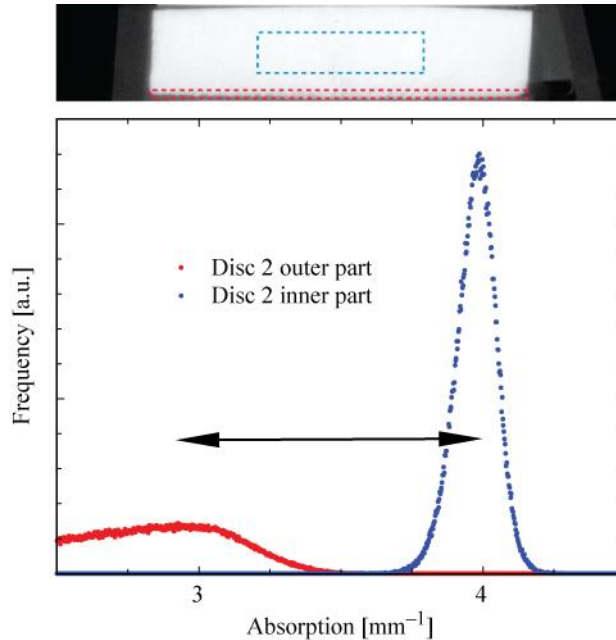


Fig. 4. For each disc, the rim region as shown by the red-colored dashed box was selected and compared with the core region (blue dashed box in the center of the disc). The related histograms can be used to quantify the absorption of rim and core. The relative peak positions were regarded as characteristic.

Note that the histogram of the core (Disc 2) exhibits a rather symmetric peak, which gives rise to well-defined values for the peak position. The histogram of the rim region shows a broad distribution, which cannot be reasonably fitted by one Gaussian.

Table 2. Relative peak positions of top and bottom side with respect to the inner part of the discs.

	Top side	Bottom side
Disc 1	85%	96%
Disc 2	91%	75%
Disc 3	86%	86%
Disc 4	86%	87%

### 3.2 Characterization of the dentin microstructure by SR $\mu$ CT

Standard SR $\mu$ CT allows imaging dentin tubules.<sup>20, 21</sup> Nevertheless, the morphology of dentin is usually described on the nanometer scale and, therefore, not easy accessible by  $\mu$ CT.<sup>22</sup> The etching, however, could selectively remove certain components so that the nanoscopic structure and characteristic features such as anisotropy become clearly visible even on the micrometer level.

Figure 5 demonstrates that characteristic microstructures of dentin can be uncovered by means of SR $\mu$ CT-measurements. The frontal and the sagittal slices of Disc 2 (top images in Fig. 5) underline that one side of the disc is rough and displays protrusions with a periodicity of roughly 50  $\mu$ m. The protrusions on the surface correlate with the density modulations, which, although hardly visible in the frontal view, are quite clear in the sagittal slice. The protrusions are related to the higher absorbing features inside the disc, implying that the lower absorbing features are preferentially etched by the citric acid treatment.

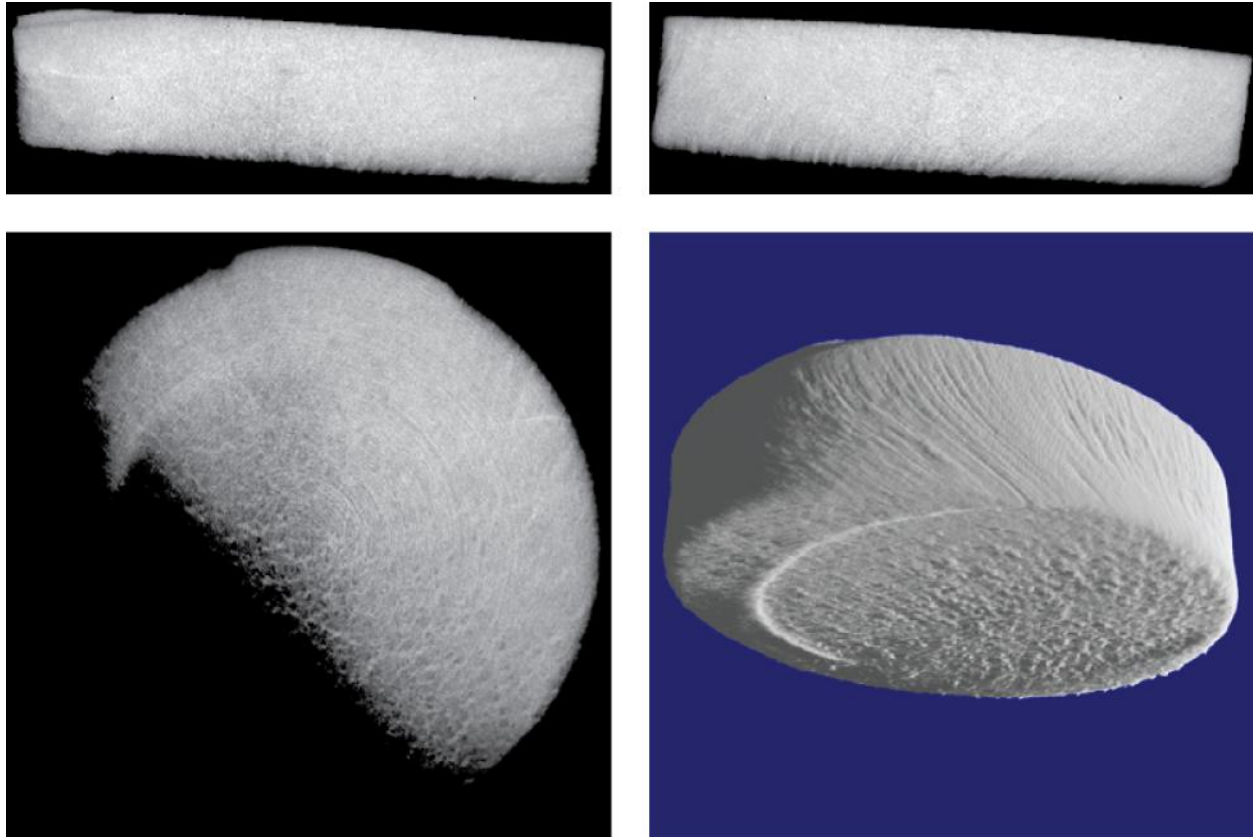


Fig. 5. The 3 slices (frontal, sagittal and axial virtual cuts) and the 3D representation of the 4 mm wide Disc 2 clearly show the anisotropy of the dentin and the tubular structure. The surface roughness on the micrometer scale relates to the X-ray absorption modulations in the bulk as seen best for the sagittal slice (top, right).

The elongated features characterized by the higher local absorption values (bright) in the axial and sagittal slices are also present in the axial slice (second line, left). Here, they do not appear elongated but rather as a net-like microstructure. These observations correlate well with the 3D surface representation shown in Figure 5, second line on the right. On the side of the cylindrically shaped sample and near the partial ring (that originates from Disc 3), the approximately 50  $\mu\text{m}$  wide features are elongated, while the other part of the surface displays a net-like microstructure.

#### 4. DISCUSSION

With respect to polymer containers and saline, dentin exhibits a high X-ray absorption that can be measured in a liquid environment avoiding the dehydration of specimens and for subsequent intensity-based segmentation by thresholding.

It is established that SR $\mu$ CT provides well-defined quantities, namely the local X-ray absorption at the selected photon energy. Consequently, the method permits conclusions about spatial variations on material's density and composition. In the case of dentin specimens, it is useful to determine such variations within an individual tooth, between different teeth of one patient or of different patients. Although the present preliminary study only included 4 discs, our results demonstrate that such variations are clearly detectable and can be quantitatively assessed by SR $\mu$ CT.

Since the mineral content of dentin can fluctuate considerably, the de-mineralization studies have to be calibrated in an appropriate manner. Here, we have used the core part of the specimen as a standard assuming that the acid acts on the surface of the specimens and does not react with this core. Because of the non-destructive character of SR $\mu$ CT, one could imagine use of only one disc for the different steps of the procedure, i.e. native state, after the acidic treatment (etching), and after different periods of re-mineralization. The disadvantage of such an approach is the need for interrupted beamtime at the synchrotron, which is difficult to organize.



The study elucidates that the degree of mineralization on the top and the bottom of the disc can differ much more than 10%. This can be understood by the choice of the extraction site. The dentin density and composition can significantly vary from pulp to enamel junctions. Therefore, the extraction site has to be carefully selected. This is not an easy task and seems to require quantitative, non-destructive measurements to determine an optimized area prior to cutting. Here, high-density resolution  $\mu$ CT could be a powerful tool.

Different scenarios are known to describe the acidic etching. First, the acid could penetrate into the material and preferentially dissolve the calcium phosphate phases. In the present study we have not observed such behavior. This can be understood by the remarkable buffer capacity of dentin.<sup>23</sup> Therefore, de-mineralization in the deeper layers of specimens was not found. Second, the acid could act directly on the specimen surface. Because of the composite structure of dentin and variations in the composition and density, the acid is expected to selectively etch certain components. Hence, the surface becomes rough and reveals the characteristic microstructure as illustrated by the three-dimensional surface representation in Figure 6 (top disc native – Disc 1, second disc etched – Disc 2). In Figure 5, where Disc 2 is represented, one recognizes from the frontal view and especially from the sagittal view that the less X-ray opaque components were preferentially removed by the etching treatment. This means that the microstructure seen on the surface correlates to the density or composition variations in the bulk material.

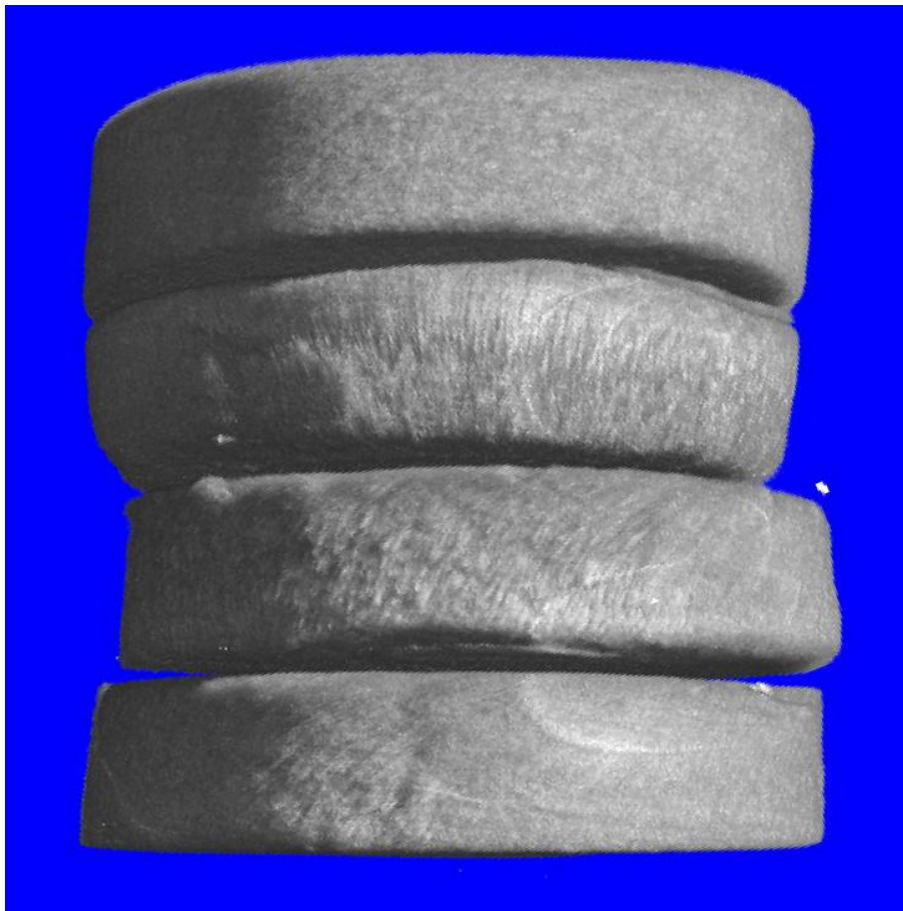


Fig. 6. The 3D representation of the dentin discs (Disk 1 to 4 from top to bottom) shows that the native disc (Disc 1) exhibits the lowest roughness on the micrometer scale. Etching results in high and anisotropic roughness, which is significantly reduced by the re-mineralization (Disc 3 after 1 d and Disc 4 after 7 d of treatment).

The restriction of the etching onto the surface region also suggests that the re-mineralization is also limited to the skin of the discs. This could be perceived in Figure 6. The surface roughness of Disc 3 and Disc 4 appears less prominent than that of Disc 2. The discs treated with the bio-active glass suspension show the expected time-dependence in the degree of re-mineralization. Quite clear initial signs of re-mineralization are present already after 24 h of incubation, whereas the disc incubated for 7 d demonstrates an appearance almost comparable to the native disc (Disc 1).

## 5. CONCLUSIONS

The composition and/or the density of dentin depend on its location within the individual tooth. Consequently, the site of extraction has to be carefully selected. High-density resolution  $\mu$ CT is expected to meaningfully support this selection. As the dentin belongs to the biological composite materials, a sequential investigation of one specimen in a non-destructive way has to be preferred with respect to direct comparison between different discs. Using different discs, one can analyze the core part of the specimen as the reference for calibration purposes. Here, however, the changes from pulp to enamel junctions have to be considered, which decreases the measurement accuracy.

Etching (de-mineralization) and bio-active nanoparticle treatment (re-mineralization) of the dentine discs are mainly surface phenomena. Therefore, surface sensitive methods such as atomic force microscopy could be better suited to reveal such roughness on the micro- and nanometer scales, quantitatively. SR $\mu$ CT can create the link between the results of such surface studies and the bulk microstructure. Therefore, SR $\mu$ CT contributes to the search for better patient treatments in dentistry.

## ACKNOWLEDGEMENTS

The authors gratefully acknowledge for the beamtime at HASYLAB at DESY, Hamburg, Germany and for improving the English of the manuscript by William Wishart.

## REFERENCES

- [1] Hench, L.L. and Paschall, H.A., "Direct chemical bond of bioactive glass-ceramic materials to bone and muscle", *J Biomed Mater Res* 7 (3), 25-42 (1973).
- [2] Gillam, D.G., Tang, J.Y., Mordan, N.J. and Newman, H.N., "The effects of a novel Bioglass dentifrice on dentine sensitivity: a scanning electron microscopy investigation", *J Oral Rehabil* 29 (4), 305-313 (2002).
- [3] Oguntebi, B., Clark, A. and Wilson, J., "Pulp capping with Bioglass and autologous demineralized dentin in miniature swine", *J Dent Res* 72 (2), 484-489 (1993).
- [4] Zamet, J.S., Darbar, U.R., Griffiths, G.S., Bulman, J.S., Bragger, U., Burgin, W. and Newman, H.N., "Particulate bioglass as a grafting material in the treatment of periodontal intrabony defects", *J Clin Periodontol* 24 (6), 410-418 (1997).
- [5] Pashley, D.H., "Dentin: a dynamic substrate--a review", *Scanning Microsc* 3 (1), 161-174; discussion 174-166 (1989).
- [6] Stoor, P., Soderling, E. and Salonen, J.I., "Antibacterial effects of a bioactive glass paste on oral microorganisms", *Acta Odontol Scand* 56 (3), 161-165 (1998).
- [7] Zehnder, M., Waltimo, T., Sener, B. and Soderling, E., "Dentin enhances the effectiveness of bioactive glass S53P4 against a strain of *Enterococcus faecalis*", *Oral Surg Oral Med Oral Pathol Oral Radiol Endod* 101 (4), 530-535 (2006).
- [8] Allan, I., Newman, H. and Wilson, M., "Antibacterial activity of particulate bioglass against supra- and subgingival bacteria", *Biomaterials* 22 (12), 1683-1687 (2001).
- [9] Sepulveda, P., Jones, J.R. and Hench, L.L., "In vitro dissolution of melt-derived 45S5 and sol-gel derived 58S bioactive glasses", *J Biomed Mater Res* 61 (2), 301-311 (2002).
- [10] Waltimo, T., Brunner, T.J., Vollenweider, M., Stark, W.J. and Zehnder, M., "Antimicrobial effect of nanometric bioactive glass 45S5", *J Dent Res* 86 (8), 754-757 (2007).



- [11] Forsback, A.P., Areva, S. and Salonen, J.I., "Mineralization of dentin induced by treatment with bioactive glass S53P4 in vitro", *Acta Odontol Scand* 62 (1), 14-20 (2004).
- [12] Kangasniemi, I.M., Vedel, E., de Blick-Hogerworst, J., Yli-Urpo, A.U. and de Groot, K., "Dissolution and scanning electron microscopic studies of Ca,P particle-containing bioactive glasses", *J Biomed Mater Res* 27 (10), 1225-1233 (1993).
- [13] Beckmann, F., Donath, T., Dose, T., Lippmann, T., Martins, R.V., Metge, J. and Schreyer, A., "Microtomography using synchrotron radiation at DESY: current status and future developments (Proceedings Paper)," in *Developments in X-ray Tomography IV* Bonse, U., Ed., pp. 1-10, SPIE, San Diego, USA (2004).
- [14] Müller, B., Bernhardt, R., Weitkamp, T., Beckmann, F., Bräuer, R., Schurigt, U., Schrott-Fischer, A., Glueckert, R., Ney, M., Beleites, T., Jolly, C. and Scharnweber, D., "Morphology of bony tissues and implants uncovered by high-resolution tomographic imaging", *Int J Mat Res* 98 (7), 613-621 (2007).
- [15] Kak, A.C. and Slaney, M., [Principles of Computerized Tomographic Imaging], IEEE Press, New York (1988).
- [16] Müller, B., Thurner, P., Beckmann, F., Weitkamp, T., Rau, C., Bernhardt, R., Karamuk, E., Eckert, L., Brandt, J., Buchloh, S., Wintermantel, E., Scharnweber, D. and Worch, H., "Non-destructive three-dimensional evaluation of biocompatible materials by microtomography using synchrotron radiation," in *Developments in X-ray Tomography III* Bonse, U., Ed., pp. 178-188, SPIE, San Diego, USA (2001).
- [17] Grodzins, L., "Optimum energies for X-ray transmission tomography of small samples", *Nucl. Instrum. Meth.* 206, S41-S45 (1983).
- [18] Thurner, P., Beckmann, F. and Müller, B., "An optimization procedure for spatial and density resolution in hard X-ray micro-computed tomography", *Nucl. Instrum. Meth.* 225 (4), 599-603 (2004).
- [19] Müller, B., Beckmann, F., Huser, M., Maspero, F., Székely, G., Ruffieux, K., Thurner, P. and Wintermantel, E., "Non-destructive three-dimensional evaluation of a polymer sponge by micro-tomography using synchrotron radiation", *Biomolecular Engineering* 19, 73-78 (2002).
- [20] Stock, S.R., Vieira, A.E.M., Delbem, A.C.B., Cannon, M.L., Xiao, X. and Carlo, F.D., "Synchrotron microComputed Tomography of the mature bovine dentinoenamel junction", *J. Structural Biol.* 161 (2), 162-171 (2008).
- [21] Zabler, S., Cloetens, P. and Zaslansky, P., "Fresnel-propagated submicrometer x-ray imaging of water-immersed tooth dentin", *Optics Lett.* 32 (20), 2987-2989 (2007).
- [22] Tavares Coutinho, E., Moraes d'Almeida, J.R. and Paciornik, S., "Evaluation of Microstructural Parameters of Human Dentin by Digital Image Analysis", *Mater. Res.* 10 (2), 153-159 (2007).
- [23] Haapasalo, M., Qian, W., Portenier, I. and Waltimo, T., "Effects of dentin on the antimicrobial properties of endodontic medicaments", *J. Endod.* 33, 917-925 (2007).